MARTIN MARIETTA ENERGY SYSTEMS LIBRARIES
3 4456 0365455 1

ORNL-3444
UC-28 – Particle Accelerators and
High-Voltage Machines
TID-4500 (26th ed.)

PHASE MOTION OF IONS IN ISOCHRONOUS CYCLOTRONS

F. M. Russell

CENTRAL RESEARCH LIBRARY
DOCUMENT COLLECTION
LIBRARY LOAN COPY
DO NOT TRANSFER TO ANOTHER PERSON
If you wish someone else to see this document, send in name with document and the library will arrange a loan.

OAK RIDGE NATIONAL LABORATORY
operated by
UNION CARBIDE CORPORATION
for the
U.S. ATOMIC ENERGY COMMISSION

Printed in USA. Price: $0.75 Available from the
Office of Technical Services
U. S. Department of Commerce
Washington 25, D. C.

LEGAL NOTICE

This report was prepared as an account of Government sponsored work. Neither the United States, nor the Commission, nor any person acting on behalf of the Commission:

A. Makes any warranty or representation, expressed or implied, with respect to the accuracy, completeness, or usefulness of the information contained in this report, or that the use of any information, apparatus, method, or process disclosed in this report may not infringe privately owned rights; or

B. Assumes any liabilities with respect to the use of, or for damages resulting from the use of any information, apparatus, method, or process disclosed in this report.

As used in the above, "person acting on behalf of the Commission" includes any employee or contractor of the Commission, or employee of such contractor, to the extent that such employee or contractor of the Commission, or employee of such contractor prepares, disseminates, or provides access to, any information pursuant to his employment or contract with the Commission, or his employment with such contractor.

ORNL-3444

Contract No. W-7405-eng-26

ELECTRONUCLEAR DIVISION

PHASE MOTION OF IONS IN ISOCHRONOUS CYCLOTRONS

F. M. Russell

January 1963

FEBRUARY 1964

OAK RIDGE NATIONAL LABORATORY
Oak Ridge, Tennessee
Operated by
UNION CARBIDE CORPORATION
for the
U. S. ATOMIC ENERGY COMMISSION

MARTIN MARIETTA ENERGY SYSTEMS LIBRARIES

3 4456 0365455 1

Contents

Abstract 1

1. Introduction 1
2. The Non-Radial Gap 2
3. The Isophase Curve 5
4. Non-Uniform Gap Voltages 7
5. Spread in Energy 10
6. Curvature of Isophase Line 12
7. Field Imperfections 13
8. Random Errors 15
9. Gap Voltage Variations 16
10. The Gap Spiral 16
11. Radial Stability 20
12. Practical Applications 21
13. Phase Control by Additional Electrodes 24

Appendix I: The Mean Orbit 27

Appendix II: Random Errors 29

Appendix III: Field Perturbations 30

Appendix IV: Magnetic Fields Associated with RF Cavities . . . 31

References 32

Phase Motion of Ions in Isochronous Cyclotrons

F. M. Russell*

Oak Ridge National Laboratory

Abstract

The motion in phase of ions in isochronous cyclotrons possessing non-radial accelerating gaps is examined and it is shown that under certain conditions a quasi-phase-stable state is possible. By differentially modulating the gap voltage with radius in adjacent gaps and slightly perturbing the magnetic field it is possible to focus ions upon a chosen phase angle. The major advantages associated with such a scheme are the reductions in sensitivity of the phase of ions to errors in the magnetic field and to gap voltage variations. The possibility of controlling the phases of ions by using extra electrodes also is examined; it is shown that large phase compression could be achieved under certain conditions.

---

1. Introduction

An attempt is made in this paper to examine the effect of non-radial accelerating gaps upon the motion in phase of ions in a cyclotron with an isochronous magnetic field. In conventional cyclotrons, the phase of the orbiting ions relative to that of the accelerating gap voltage varies as a result of the relativistic increase in mass of ions with increasing energy and also from the requirement for axial stability of ion motion, namely, a decreasing magnetic field strength with increasing radius[1]. However, by introducing azimuthal variations in the strength of the magnetic field, it is possible to eliminate the phase

---

*Visiting scientist, Electronuclear Division, from Rutherford High Energy Laboratory, Harwell.

changes associated with conventional cyclotrons[2]. The phase of an ion in an isochronous cyclotron ought, therefore, to remain unchanged during the process of acceleration.

A design study for a large isochronous cyclotron undertaken at Oak Ridge[3] calls for the use of cavities instead of the more usual 180°-dee arrangement for the accelerating electrode system. Owing to the unusual design of the magnet[4] for the proposed machine, the accelerating gaps formed by these cavities would be non-radial. The circulating ions would then experience a radial force during each crossing of the accelerating gaps caused by the radial component of the electric field in the gaps. Further, the magnitude and direction of this force would be dependent on the phase of the ions at each gap crossing.

It will be shown that in the special case where the voltage across the accelerating gap is independent of radius or there is no differential variation of the gap voltage in adjacent (in azimuth) gaps, then the radial electric forces produce no net effect upon the phases of the ions. The more general case in which the gap voltage varies with the radius is then examined, and it is shown that some measure of control over the phase of the ions can be achieved. In conclusion, some possible practical applications of this effect are examined in relation to large isochronous cyclotrons.

2. The Non-Radial Gap

Let the gap vary in position according to the law

$$\theta = G(\rho) , \tag{1}$$

where G is a function only of ρ . From Fig. 1, the radial component of the electric field in the gap is

$$\xi_r = \frac{V_g}{S_g} \sin \sigma , \tag{2}$$

where:

$$\tan \sigma = \rho \frac{d\theta}{d\rho} \quad . \tag{3}$$

Because the gap is spiraled, the effective width of the gap is greater than the actual width, in the ratio 1: $1/\cos \sigma$; fringe field effects are neglected.

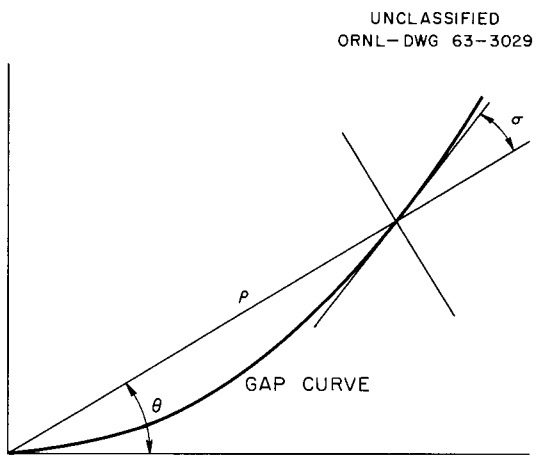

Fig. 1. Coordinates describing the gap spiral and angle σ.

The radial impulses experienced by a circulating ion can be Fourier analyzed to give a term, F_r, independent of the azimuth, and a series of harmonic driving terms, D_n, where n is the harmonic number. If there are N gaps equally distributed around the machine, then the magnitude of the first force term is

$$F_r = \frac{Ne\,V_g}{2\pi\ \rho\, r_0} \tan \sigma \ , \tag{4}$$

and from Eq. (3),

$$F_r = \frac{Ne\,V_g}{2\pi\, r_0} \frac{d\theta}{d\rho} \quad . \tag{5}$$

The magnitudes of the harmonic driving force terms are given by

$$D_n = \frac{NA\ 2 \sin (n\alpha\pi)}{\pi n} \cos n\ \omega_0 t \ , \tag{6}$$

where:

$$A = \frac{eV_g}{S_g} \sin \sigma \ , \tag{7}$$

$$a = \frac{S_g}{2\pi \ \rho r_0 \cos \sigma} \ , \tag{8}$$

and

$$n = Nm, \quad m = 1, 2, \ldots \tag{9}$$

The angular frequency ω_0 is defined as c/r_0, that is, the cyclotron angular frequency.

The effect of the force term F_r upon an orbiting ion can be represented by a change in the strength of the magnetic field, averaged over the equilibrium orbit. For simplicity, a smooth magnetic field approximation is used here; the effect of the D_n terms upon the orbits is considered in Appendix I. The basic equation for an isochronous cyclotron,

$$\hat{B}_{iso} ev = \frac{(E_0 + T)}{r_0} \ , \tag{10}$$

combined with Eq. (5), gives

$$\frac{\Delta\hat{B}}{\hat{B}_{iso}} = \frac{NeV_g}{2\pi \rho \ (E_0+T)} \ \frac{d\theta}{d\rho} \ , \tag{11}$$

where $\Delta\hat{B}$ is the equivalent change in the magnetic field produced by the radial electric force term. By the use of the isochronism condition relating total energy to $\hat{B}_{iso}$, Eq. (11) can be rewritten as

$$\frac{\Delta\hat{B}}{\hat{B}_0} = \frac{NeV_g}{2\pi E_0} \left(\frac{1}{\rho} \ \frac{d\theta}{d\rho}\right) \ . \tag{12}$$

From this expression the magnitude of the radial term can easily be found for a given spiral law. For example, for the particular spiral law[3] $\theta = \rho^2$ and with a maximum energy gain of 1 MeV/turn, $\Delta\hat{B}/\hat{B}_0$ is approximately 3.3×10^{-4}.

3. The Isophase Curve

Consider the instantaneous positions occupied by an ion after successive time intervals equal to the cyclotron period. The locus of these points is called here the "isophase curve". If the condition of isochronism is to be maintained, then the isophase curve must either delineate the curve of the gap or be related to that curve by a constant phase angle.

Let the magnetic field be designed for isochronism so that the isophase curve is purely radial. The effect of any radial electric force is to change the period of rotation of the ions and, so, to distort isophase curve from the initial radial line.

For an ion of given momentum the product $\hat{B}\rho$ is constant and so the change in ρ caused by the equivalent magnetic field change $\Delta\hat{B}$ is found from

$$\hat{B}_{iso}\,\rho = \left(\hat{B}_{iso} + \Delta\hat{B} + \delta\rho \frac{\hat{B}_{iso}}{d\rho}\right)(\rho + \delta\rho), \tag{13}$$

which gives, neglecting second order terms,

$$\frac{\delta\rho}{\rho} = -(1-\rho^2)^{3/2}\,\frac{\Delta\hat{B}}{\hat{B}_0}. \tag{14}$$

Hence, the shift in phase per turn caused by the radial electric force is

$$\frac{2\pi\,\delta\rho}{\rho} = \frac{NeV_g}{E_0}(1-\rho^2)^{3/2}\,\frac{1}{\rho}\,\frac{d\theta}{d\rho}\cos\Psi, \tag{15}$$

where Ψ is the phase of the ion relative to the gap voltage.

Now, each turn the ion will gain energy to the amount ΔT, where

$$\Delta T = NeV_g \cos\Psi, \tag{16}$$

and, since the rate of change of ρ with energy for an isochronous cyclotron is given by

$$\frac{d\rho}{dT} = \frac{(1-\rho^2)^{3/2}}{\rho E_0}, \tag{17}$$

it follows that the increase in ρ per turn is

$$\Delta \rho = \frac{(1 - \rho^2)^{3/2}}{\rho \; E_0} \; NeV_g \cos \Psi \quad . \tag{18}$$

From Fig. 2, in which the line AA' represents a part of the gap curve and 0 represents the machine center, the change in phase angle per turn required to make the ion cross the gap without suffering any phase shift relative to the gap voltage is

$$-\Delta \theta = \Delta \rho \frac{\partial \theta}{\partial \rho} \quad . \tag{19}$$

Substitution for $\Delta \rho$ from Eq. (18) results in an expression which is identical to that given in Eq. (15). Hence, the radial electric force produced by the gap exactly compensates for the phase shift required per turn to maintain the condition of isochronism[5]. The isophase curve is identical, therefore, with the gap curve except for the possibility of a constant angular displacement.

UNCLASSIFIED
ORNL-DWG 63-3030

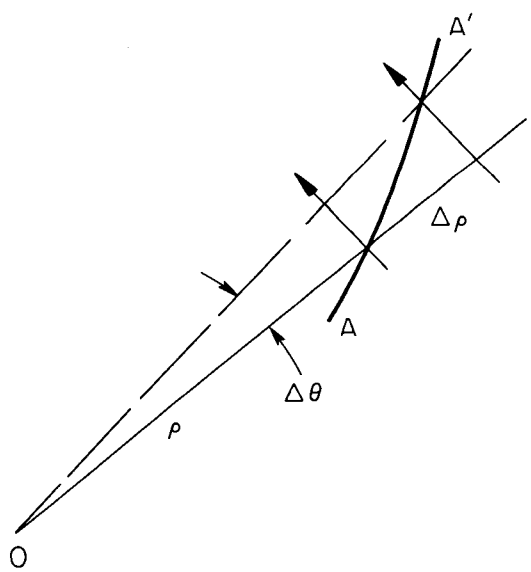

Fig. 2. Diagram illustrating the change in angle in azimuth $\Delta \theta$ of the gap as the orbit radius is increased.

4. Non-Uniform Gap Voltages

In the preceding section the isophase and gap curves were shown to be similar. However, if the amplitude of the gap voltage is caused to vary with radius, then the curves can become dissimilar. In Fig. 3 two spiral gaps are indicated by the curves OA and OB. Let the voltage amplitude in gap OA decrease with increasing radius and in gap OB increase with radius. In addition, let the voltages in the two gaps be in phase. An ion rotating in the manner indicated would experience accelerations at both gaps. At small radii, the major part of the acceleration would occur at the OA gap, but at large radii the conditions would be reversed and the gap OB would contribute most to the energy gain.

UNCLASSIFIED
ORNL-LR-DWG 79264

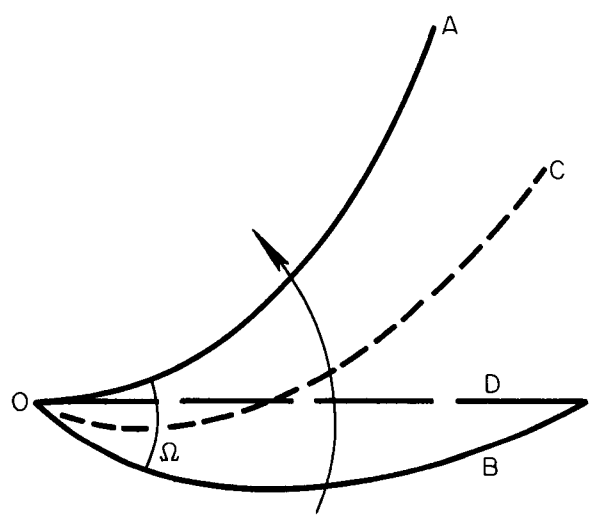

Fig. 3. Schematic diagram showing how the isophase curve OC is formed from two neighboring gaps OA and OB.

The isophase points would thus lie along some such curve as OC; by appropriately modulating the gap voltages in radius the curve could be made radial, as shown at OD. In this manner, it is possible to have a radial isophase curve yet retain the radial electric forces acting

upon an ion crossing the gap. From Fig. 4, $A_1(\rho)$ and $A_2(\rho)$ represent the amplitudes of the gap voltages at some given value of ρ .

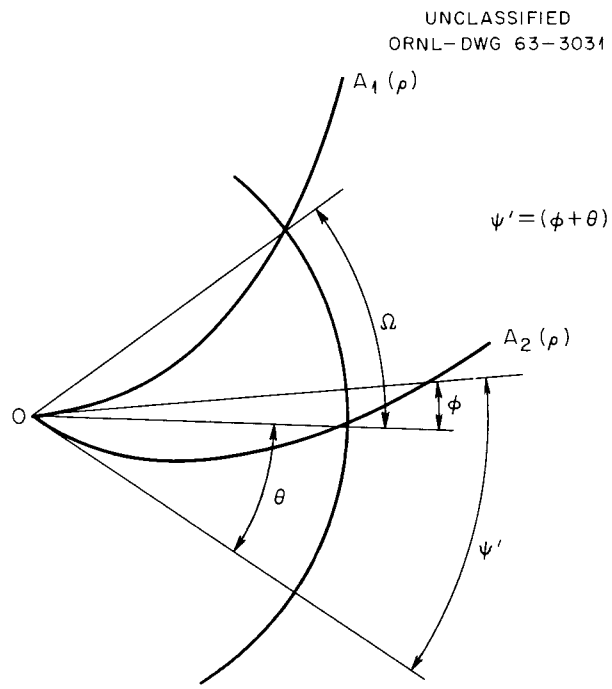

Fig. 4. Coordinates and explanation of symbols used in producing a radial isophase curve.

To maintain a radial isophase curve, the gap voltages must satisfy the condition (20)

$$\frac{A_2(\rho)}{A_1(\rho)} = \frac{\sin\Omega\,(1+\tan\Psi'\tan\theta) - \cos\Omega\,(\tan\Psi' - \tan\theta)}{(\tan\Psi' - \tan\theta)},$$

and to keep the maximum energy gain per turn independent of ρ , $A_1(\rho)$ must satisfy (21)

$$A_1(\rho) = V_g\left[\cos(\theta+\Psi) + \frac{A_2(\rho)}{A_1(\rho)}\cos(\theta+\Psi+\Omega)\right].$$

Let the voltages in adjacent gaps be modulated in the preceding way to give radial isophase lines. Further, let the magnitude of the gap voltages be such that the maximum energy gain per turn is eV_gM and independent of ρ , where M is the number of matched gap pairs ($M = N/2$).

Under this condition it is impossible to maintain the condition of isochronism independently of the phase of an ion (relative to the gap voltage). However, by suitably perturbing the originally isochronous magnetic field so as to satisfy the equation

$$\hat{B}_s = (\hat{B}_{iso} - \cos \Psi_s \Delta\hat{B}) , \tag{22}$$

the condition of isochronism is restored for ions having the phase angle Ψ_s relative to the gap voltage. Ions having phase angles other than Ψ_s would experience phase shifts each turn.

The rate of change of phase per turn for an ion having instantaneous phase angle Ψ is found from Eqs. (14) and (22), giving

$$\frac{d\Psi}{dp} = \frac{2\pi (1 - \rho^2)^{3/2} \Delta\hat{B} (\cos \Psi_s - \cos \Psi)}{\hat{B}_0} . \tag{23}$$

If the cavities are operated on the m'th harmonic of the cyclotron frequency, then the rate of change of phase is simply m times greater. Hence, by using Eqs. (12), (16), and (17), Eq. (23) can be written in the form

$$\frac{d\Psi}{d\rho} = m \left[\frac{(\cos \Psi_s - \cos \Psi)}{\cos \Psi} \right] \frac{d\theta}{d\rho} , \tag{24}$$

so that

$$I(\Psi) = \int \frac{\cos \Psi \quad d\Psi}{(\cos \Psi_s - \cos \Psi)} = m \int \left(\frac{d\theta}{d\rho}\right) d\rho . \tag{25}$$

From Eq. (1) it follows that

$$\{ I(\Psi_2, \Psi_s) - I(\Psi_1, \Psi_s) \} = m \{ G(\rho_2) - G(\rho_1) \} . \tag{26}$$

The general form of the left-hand integral, $I(\Psi)$, is shown in Fig. 5 for several values of Ψ_s.

The type of phase motion governed by Eq. (26) is illustrated for a typical spiral law in Fig. 6.

In general, ions with phases other than Ψ_s are focused towards the phase angle $(- |\Psi_s|)$, except for a critically unstable point at phase angle $(+ |\Psi_s|)$. It is apparent that the phase motion is not

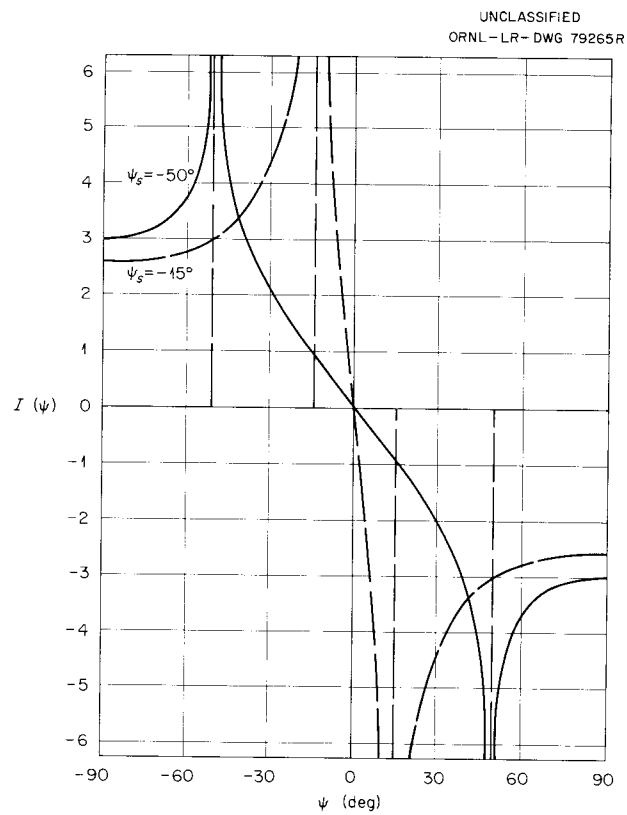

Fig. 5. Curves showing the variation of the function $I(\psi)$ with angle ψ for two values of ψ_s.

oscillatory in nature, the phase angle $(-|\Psi_s|)$ acting as a limiting stable angle.

5. Spread in Energy

A direct result of the quasi-phase-stability here described is a spread in energy of ions having common orbit radius. The limits on this energy spread are given by

$$E(\Psi) = E(\Psi_s) + \Delta\hat{B}(\cos\Psi_s - \cos\Psi)\left.\frac{dT}{d\hat{B}}\right|_{\rho\,\mathrm{const}}, \tag{27}$$

where $E(\Psi_s)$ is the total energy of an ion with phase angle Ψ_s at the appropriate value of ρ. Hence, from Eq. (11), the maximum energy

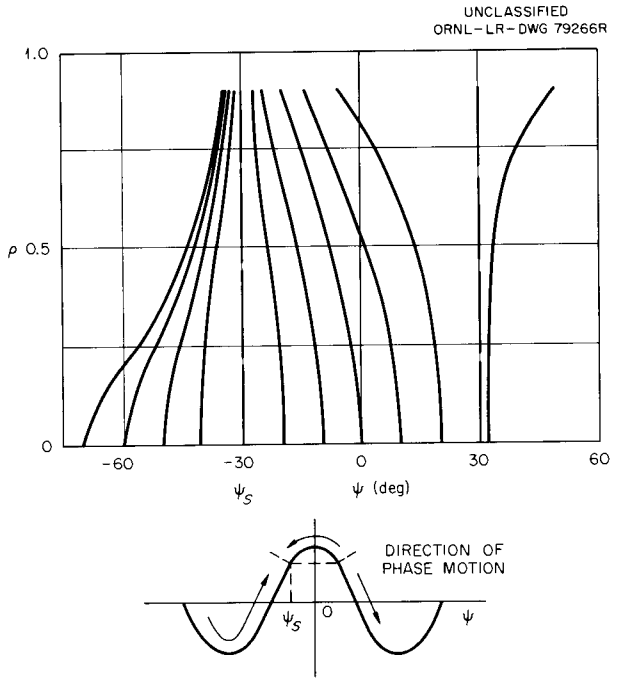

Fig. 6. The upper series of curves show the phase history of ions started with arbitrarily chosen phase angles as they are accelerated and subjected to phase focusing. The lower diagram indicates the directions of phase motions for ions of different initial phase angle.

range is

$$\Delta E = \frac{T(2E_0 3 T)}{(E_0 + T)^2} \frac{NeV_g}{\pi} \frac{1}{\rho} \frac{d\theta}{d\rho} , \tag{28}$$

which can be written in the alternative form

$$\Delta E = \frac{NeV_g}{\pi} \rho \frac{d\theta}{d\rho} . \tag{29}$$

It is apparent, however, from Fig. 6 that the convergence of the phases towards the limit Ψ_s would cause the total energy spread to be reduced progressively as ρ increases. If the useful ions at a given value of ρ are confined within the phase range ($\Psi_1 < \Psi_s$, + $|\Psi_s|$), then the total spread in energy is simply

$$\Delta E = \frac{NeV_g}{2\pi} \rho \frac{d\theta}{d\rho} (1 - \cos \Psi_1) . \tag{30}$$

In the event that the forces causing this spread in energy are made zero, the energy spread would result in an increase in the amplitude of the radial betatron oscillations. The maximum increase in amplitude is given by

$$\delta\rho \leq \rho \quad (1 - \rho^2)^{3/2} \frac{NeV_g}{2\pi E_0} \frac{1}{\rho} \frac{d\theta}{d\rho}(1 - \cos \Psi_1) \ , \qquad (31)$$

which, in most practical cases, is a negligible increase.

6. Curvature of Isophase Line

If the maximum energy gain per turn is held constant, then the maximum strength of the radial electric force also is constant and is independent of the curvature of the isophase curve. However, the magnitude of the magnetic field perturbation $\delta \hat{B}$ which is necessary to maintain isochronism at a given value of Ψ_s (when the radial electric force is present) is dependent on the curvature of the isophase line.

Let the equation to the isophase curve be

$$\theta = P(\rho) \ , \qquad (32)$$

and let the magnetic field be isochronous. From Eqs. (18) and (19) the required change of phase per turn necessary to fit the isophase curve is

$$\Psi_i' = \frac{d\Psi}{dp} = -(1 - \rho^2)^{3/2} \frac{NeV_g}{E_0} \cos \Psi \frac{1}{\rho} \frac{dP(\rho)}{d\rho} . \qquad (33)$$

The actual phase change per turn produced by the radial electric force is given by Eq. (15) and so the residual phase change per turn is

$$\Psi_r' = (1 - \rho^2)^{3/2} \frac{NeV_g}{E_0} \cos \Psi \left[\left(\frac{1}{\rho} \frac{dP(\rho)}{d\rho}\right) - \left(\frac{1}{\rho} \frac{dG(\rho)}{d\rho}\right)\right]. \qquad (34)$$

If the isophase and gap curves are identical, then Ψ_r' is zero and corresponds to the situation in which the gap voltage is independent of radius. Perturbation of the magnetic field to the extent $\delta \hat{B}(\rho)$ introduces an additional phase shift per turn and the phase equation

becomes

$$\Psi' = (1 - \rho^2)^{3/2} \left\{ 2\pi \frac{\delta \hat{B}(\rho)}{\hat{B}_0} \right.$$

$$\left. + \frac{NeV_g}{E_0} \cos \Psi \left[\left(\frac{1}{\rho} \frac{dP(\rho)}{d\rho} \right) - \left(\frac{1}{\rho} \frac{dG(\rho)}{d\rho} \right) \right] \right\}. \tag{35}$$

This is the generalized form of Eq. (23). Let Ψ' be zero for a given value of Ψ, say Ψ_s, then Eq. (35) becomes

$$\Psi' = (1 - \rho^2)^{3/2} \frac{NeV_g}{E_0} \left[\left(\frac{1}{\rho} \frac{dG(\rho)}{d\rho} \right) - \left(\frac{1}{\rho} \frac{dP(\rho)}{d\rho} \right) \right] (\cos \Psi_s - \cos \Psi), \tag{36}$$

where the magnetic field correction term is

$$\frac{\delta \hat{B}(\rho)}{\hat{B}_0} = + \frac{NeV_g}{2\pi E_0} \cos \Psi_s \left[\left(\frac{1}{\rho} \frac{dG(\rho)}{d\rho} \right) - \left(\frac{1}{\rho} \frac{dP(\rho)}{d\rho} \right) \right]. \tag{37}$$

Equation (36) indicates how the shape of the isophase curve affects Ψ'; as the isophase curve is bent away from the gap, against the direction of ion rotation, the magnitude of the phase focusing term increases.

7. Field Imperfections

The effect upon the phase equation of the mean magnetic field departing from the desired dependence upon ρ can be found by including in Eq. (36) the appropriate Ψ' term produced by the field error $\hat{b}(\rho)$. Including the possibility of harmonic operation, Eq. (36) then becomes

$$\Psi' = m (1 - \rho^2)^{3/2} \left\{ \frac{NeV_g}{E_0} \left[\frac{1}{\rho} \frac{dG(\rho)}{d\rho} - \frac{1}{\rho} \frac{dP(\rho)}{d\rho} \right] \right.$$

$$\left. \times (\cos \Psi_s - \cos \Psi) + \frac{2\pi \hat{b}(\rho)}{\hat{B}_0} \right\}, \tag{38}$$

which can be written in the form

$$\Psi' = m(1-\rho^2)^{3/2}\frac{NeV_g}{E_0}\left[G'(\rho) - P'(\rho)\right](\cos\Psi_s' - \cos\Psi), \tag{39}$$

where

$$\cos\Psi_s' = \cos\Psi_s + \frac{2\pi\hat{b}(\rho)}{\hat{B}_0}\frac{E_0}{NeV_g}\left[G'(\rho) - P'(\rho)\right]^{-1}. \tag{40}$$

The effect of the mean field error, therefore, is to change the effective value of the limiting phase angle from Ψ_s to Ψ_s'. The expression corresponding to Eq. (26) now becomes

$$\left\{I(\Psi_s', \Psi_2) - I(\Psi_s', \Psi_1)\right\} = m\left\{G(\rho_2) + P(\rho_1) - G(\rho_1) - P(\rho_1)\right\}. \tag{41}$$

Eqs. (40) and (41) can be used to determine the maximum permissible mean field error, of constant sign, that could be tolerated in any given case.

It is of interest to compare the phase histories of ions subject to a constant field error in a cyclotron under normal conditions and under conditions giving phase focusing.

Shown in Fig. 7 are curves for ions starting at different phases and subject to a constant field error of $\hat{B}_0/10^4$ in a machine with the gap and isophase curves coincident. The corresponding curves under conditions of phase focusing are shown in Fig. 8. The possibility of phase bunching at the center of a cyclotron, here omitted, can readily be included. Consider only those ions with starting phases lying between $\pm 30°$; it is apparent that with phase control the ions are considerably less distributed in phase at large radii than when such control is absent.

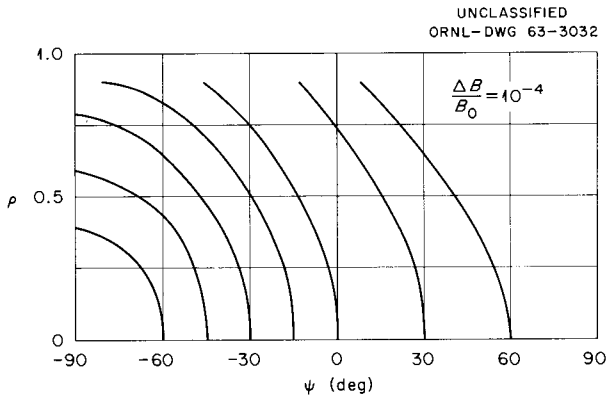

Fig. 7. Phase history of ions subject to a uniform field error in an otherwise perfect magnetic field.

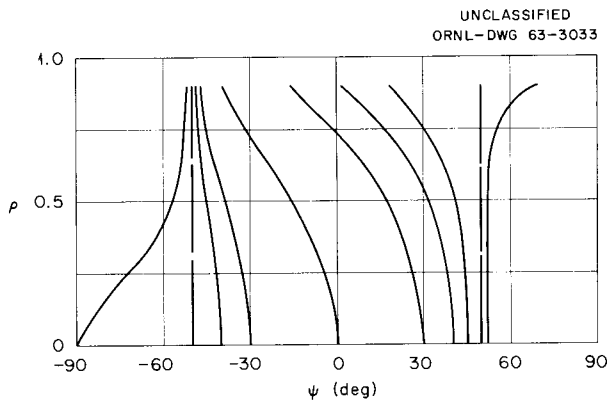

Fig. 8. Phase history of ions subject to both a uniform field error and phase focusing in an otherwise perfect field.

8. Random Errors

In practice the actual magnetic field used in an isochronous cyclotron will show deviations from the ideal field. Obviously, in general it is not possible to predict either the magnitude or sign of such errors. Further, there are other factors which can cause changes in the phase of an ion, such as a jitter in the phase of the accelerating

voltages (perhaps caused by vibration of the accelerating electrode structures), scattering of the beam by residual gas in the vacuum chamber, and space charge forces. Whatever the cause, however, the effect can be represented as actual or equivalent magnetic field errors. The analysis given in Appendix II, although very approximate, offers some insight into the effects to be expected.

It is shown that for ions starting with zero phase angle, the probable phase angle at the orbit radius (ρr_0) is given by

$$|\sin \Psi| = \frac{m\pi E_0}{NeV_g \hat{B}_0} \; |\Delta\hat{B}| \; \rho \sqrt{\Delta(\rho^2)} \quad , \tag{42}$$

where $\Delta\hat{B}$ is the average amplitude of the magnetic field errors extending over the interval $\Delta(\rho^2)$. This expression indicates that as the magnetic field error interval is decreased, so also is the magnitude of the probable phase change. Further, the magnitude of the probable phase change increases linearly with ρ.

9. Gap Voltage Variations

It is apparent from Eq. (22) that the angle Ψ_s, together with the value of $\Delta\hat{B}$ as given by Eq. (11) determine the magnitude of the magnetic field correction term $\delta\hat{B}(\rho)$. Conversely, for a given $\delta\hat{B}(\rho)$ the product ($\cos \Psi_s \Delta\hat{B}$) is constant and, since $\Delta\hat{B}$ is directly proportional to the gap voltage, it follows that the energy gain per turn is constant for ions with phase angle Ψ_s. Consequently, the convergence of the phases towards the limit Ψ_s will mitigate the effect of gap voltage variations upon the circulating ions.

10. The Gap Spiral

It is apparent from Eq. (40) that the magnitude of the magnetic field error (which can be compensated for by the radial electric forces) is strongly dependent on the angles that the gap and the isophase curves make with the path of an ion. Since there are limits set by practical

considerations on the permissible overall spiralling of the gap and isophase curves, it is of interest to examine the effect of increasing locally the rate of spiralling, yet retaining constant overall spiral angle. The gap curves shown in Fig. 9 illustrate how the localized rate of spiralling can be increased without changing the overall spiral angle. Also indicated is the isophase curve for the particular case where the gap voltages are modulated linearly with ρ, starting at $\rho_{max}/2$. From Eq. (39) the change ΔI in the integral $I(\Psi_s, \Psi)$ can be found as ρ passes through the region of increased rate of spiralling. The associated change in phase of an ion can then be found from a plot of I against Ψ for given Ψ_s.

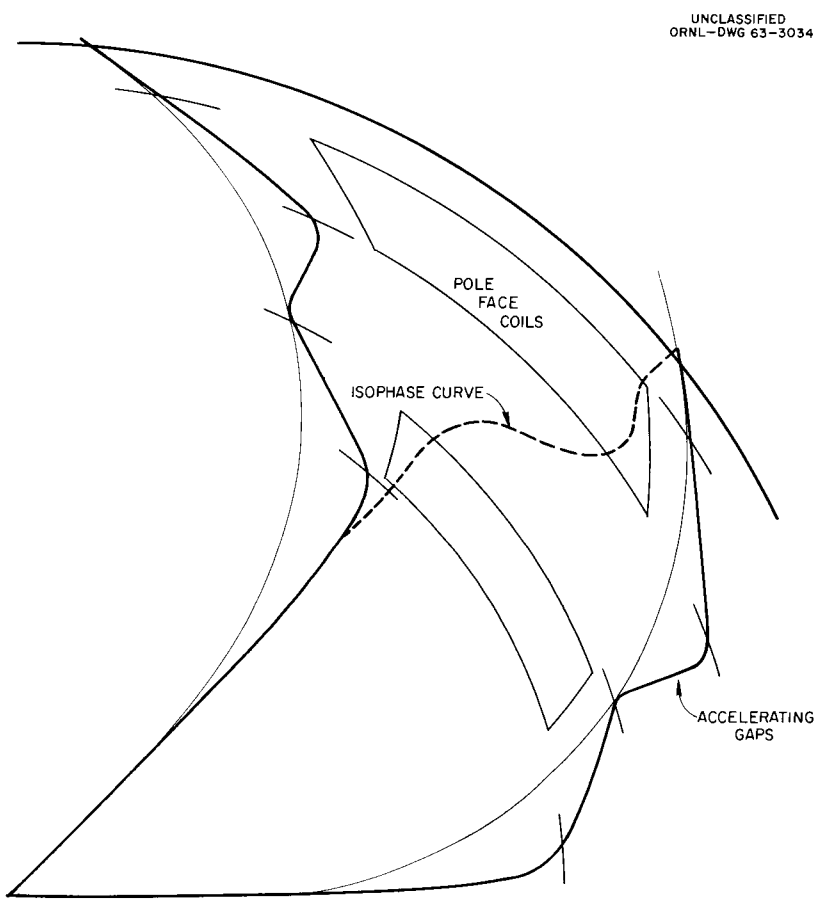

Fig. 9. Diagram illustrating how the gap spiral could be localized to small ranges in radii. Also shown is a typical isophase curve and the location of the pole-face correction coils.

Such a procedure of localization exhibits certain advantages. First, where the entire magnetic field is made isochronous initially, it is only necessary to perturb the field over limited ranges of ρ to obtain the conditions giving phase focusing, which could be achieved readily by the use of pole-face windings. Secondly, any major field errors in the vicinity of such pole-face windings could be corrected so as to permit maximum control over the phases of the ions.

A plot of the phase history of an ion for several different starting phases is shown in Fig. 7 for a constant field error of $B_0/10^4$, and in Fig. 10 for an error of $B_0/5 \times 10^3$. To illustrate the effect of localized phase focusing, the corresponding curves are given in Figs. 11 and 12 for two regions of phase focusing, with $\Delta I(\Psi_s, \Psi)$ equal to 1.0 at the

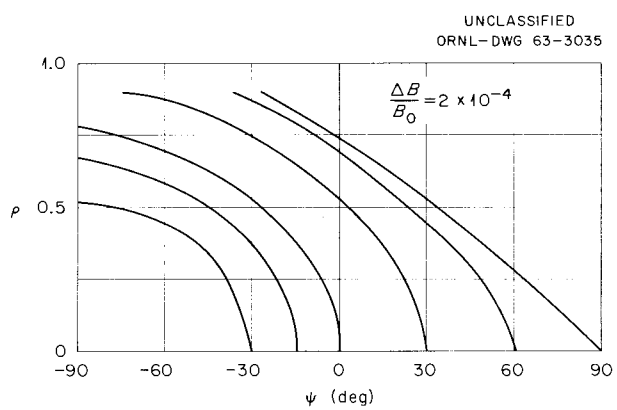

Fig. 10. Phase history of ions subject to a uniform field error.

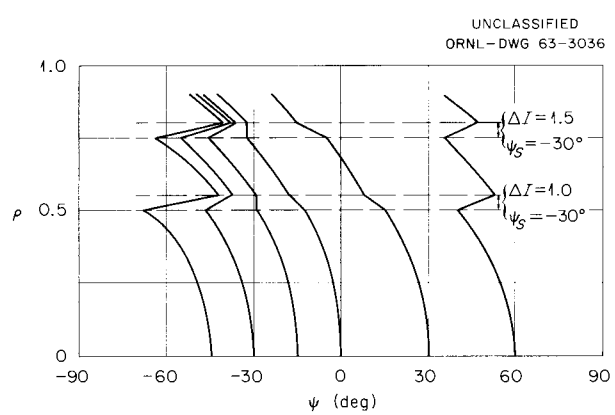

Fig. 11. Phase history of ions subject to both a uniform field error and localized phase focusing.

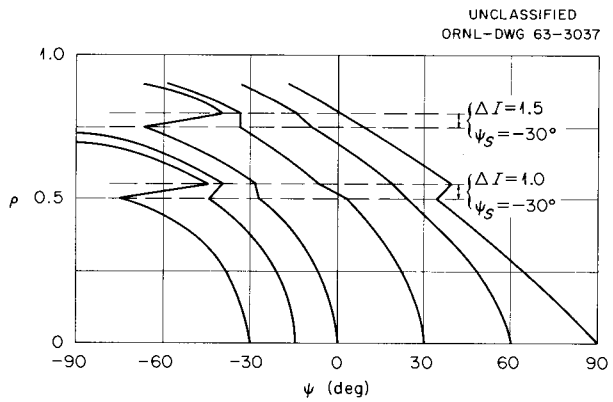

Fig. 12. Phase history of ions subject to both a uniform field error and localized phase focusing. The field error in this case is twice that of the preceding example.

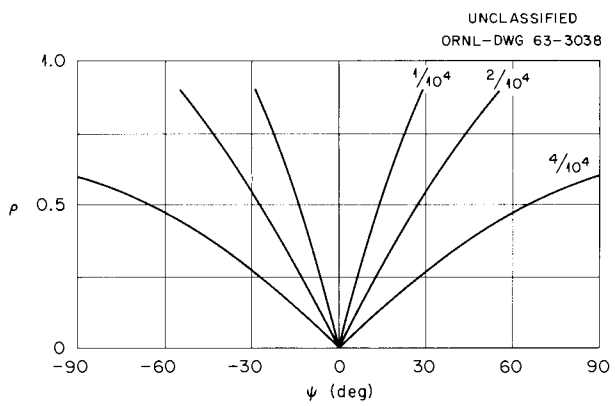

Fig. 13. Phase history showing dispersion of ions as a result of random field errors.

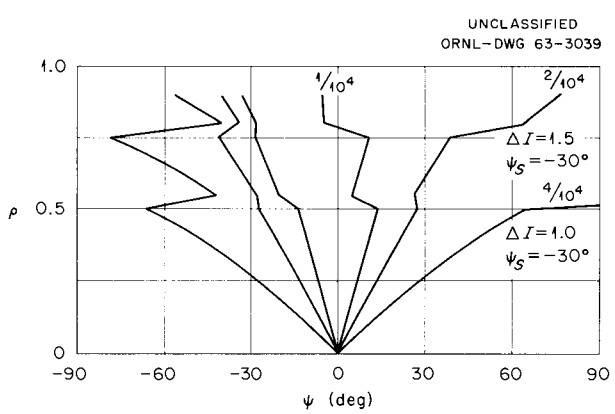

Fig. 14. Phase history where random errors are present and phase focusing is applied.

smaller radii and to 1.5 at the larger radii. It is seen that with phase focusing more ions are successfully accelerated to the full energy.

Similar results are found in the case of random errors. For example, in Fig. 13 is shown the dispersion of ions in phase according to Eq. (42). The effect of the phase control in this case, with the same values of ΔI as in the preceding example, is shown in Fig. 14. From these curves it is seen that considerably larger random errors can be tolerated when control is exercised over the phases.

11. Radial Stability

Independently of whether or not advantage is taken of the phase focusing properties obtainable in a machine using spiralled acceleration gaps, there are always harmonic driving forces which might cause difficulty in maintaining the radial stability of the beam. The ratio of the equivalent harmonic error in the magnetic field to the mean isochronous field, as found from Eqs. (6) and (10), is

$$f_n = \frac{2NA \sin(n\alpha\pi)\, r_0 \sqrt{1 - \rho^2}}{\rho E_0 n\pi} \cos(n\omega_0 t) \cos \Psi . \quad (43)$$

Thus, if $\sin(n\alpha\pi) \ll 1$, then the amplitudes of the first few harmonic terms are approximately equal and given by

$$f_n = \frac{NeV_g}{\pi E_0} \left(\frac{1}{\rho} \frac{dG(\rho)}{d\rho}\right) \sqrt{1 - \rho^2} \cos \Psi . \quad (44)$$

In accelerating systems which have symmetry about the machine axis only terms of even harmonic number are produced. The effect of these harmonic driving terms upon the amplitudes of the betatron is most pronounced when ν_r, the ratio of radial betatron to cyclotron frequencies, has a value close or equal to that corresponding to a major resonance. Of particular importance is the $\nu_r = 1$ resonance, occurring at the center of a cyclotron. An approximate expression for the maximum fractional increase in amplitude of radial oscillation caused by a second

harmonic error term at the center of a cyclotron is

$$\frac{\Delta a}{a} \simeq (e^{4\,\Delta p\, f_n} - 1) \tag{45}$$

where Δp is the number of rf cycles spent by an ion in the vicinity of the $\nu_r = 1$ resonance. In an isochronous cyclotron, the effective value of Δp is about $\sqrt{E_0/NeV_g}$. From this equation and the strength of f_n, given by Eq. (44), the increase in the amplitude of oscillation occurring after Δp cycles can be found. In practice, the increase in amplitude is quite small; for the machine discussed in reference (3) the radial amplitudes are increased by less than 10%.

At the $\nu_r = 2$ resonance, however, the increase in the radial amplitude can be large. An approximate expression[4] for the increase in amplitude at an integral imperfection resonance is

$$\delta a = \pi\, \rho\, r_0 f_n \sqrt{\Delta p}/n \ . \tag{46}$$

For the previous example, with $\rho = 0.9$ and $\Delta p = 10^3$, the maximum increase in amplitude is about 17 cm; this effectively excludes the possibility of using a two-gap system in a machine in which ν_r approaches 2. In a symmetrical four-gap system, however, the increase in the amplitude of oscillation caused by the fourth harmonic at $\nu_r = 2$ would be small.

12. Practical Applications

The relative merits of using the afore-mentioned principles in large isochronous cyclotrons are now discussed briefly. If the isophase curve is only partially straightened, then excessive loss of ions at large radii as a result of random phase shifts would be prevented. In consequence, it is probable that the background radiation intensity would be decreased and, in particular, the rate of increase in activity of the machine components would be considerably reduced.

Since at least four gaps are imperative at large radii if the $\nu_r = 2$ resonance is approached, little complication in the rf system would result from introducing radial amplitude modulation; in fact, this might ease the design of the accelerating system.

In cases where large reverse spiralling of the isophase curve is possible, considerable relaxation in the mean magnetic field tolerances could be achieved while the above-mentioned advantages are retained.

The major disadvantages are that limited pole-face windings would be necessary to adjust the mean field over one or two ranges in radii and that a small spread in energy would occur at the extraction radius.

An attractive possibility is the inclusion into a 'good' isochronous cyclotron (that is, one in which there is little slip or spread in phase) of some phase control at the high energy end, thereby stabilizing the system against small errors or drifts in the magnetic field and against variations in amplitude of the rf voltage at the gaps.

The various geometric arrangements of accelerating gaps which could provide phase control are illustrated now by application to the previously mentioned eight-sector machine[4]. In Figs. 15, 16, and 17, corresponding to operation at the first, second, and third harmonic of

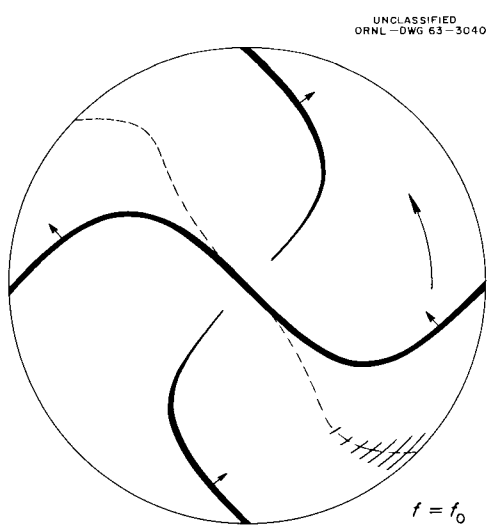

Fig. 15. Geometric arrangement of gaps to yield phase focusing when $f = f_o$. Gap voltage amplitude is indicated by thickness of gap curve. The isophase curves are also indicated.

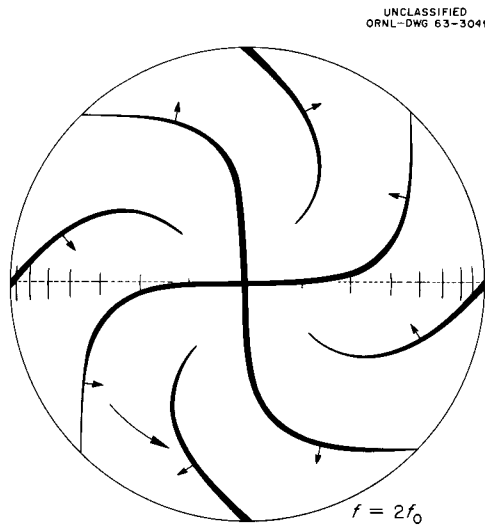

Fig. 16. Geometric arrangement of gaps to yield phase focusing when $f = 2f_o$.

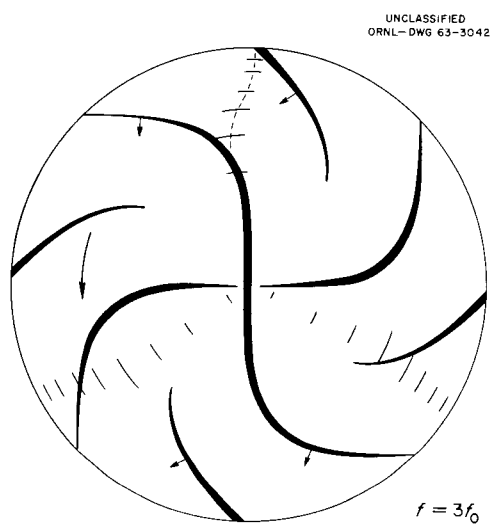

Fig. 17. Geometric arrangement of gaps to yield phase focusing when $f = 3f_o$.

the cyclotron frequency, the radial modulation of the spiral gap voltages is indicated by variation of the width of the lines representing the gaps. It is assumed in all cases shown that there must be no second harmonic error driving terms at maximum radius ($\nu_r \sim 2$). In each figure the instantaneous directions of the gap electric fields are indicated by arrows

and typical isophase curves are indicated by broken lines. Possible distributions of ions are also shown but, for simplicity of presentation, it is assumed that the error forces acting upon the ions produce only a dispersion in phase, increasing with the orbital radius.

The use of localized phase control to reduce the spread in phase of ions is shown schematically in Fig. 18. For clarity, the ion distribution without phase control is shown displaced in phase by about 90°.

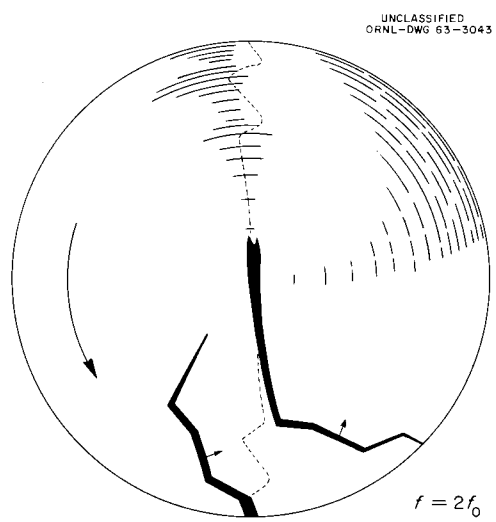

Fig. 18. Diagram showing geometric arrangement of gaps to give localized phase focusing when $f = 2f_o$. The isophase curve is also indicated. The distribution of ions in phase when subjected to random field error is illustrated, also the reduction in phase spread when localized phase focusing is applied.

13. Phase Control by Additional Electrodes

It is of interest to apply the preceding theory to a special case in which electrodes are so arranged as to emphasize the effects here examined. Assume that electrodes are used to produce a radial electric field over a length L and radial distance S and that there are N_c such systems symmetrically placed in azimuth, as indicated in Fig. 19. Let the amplitude of the voltage applied to these electrodes be V_c and let the frequency of the signal be h times that of the main rf.

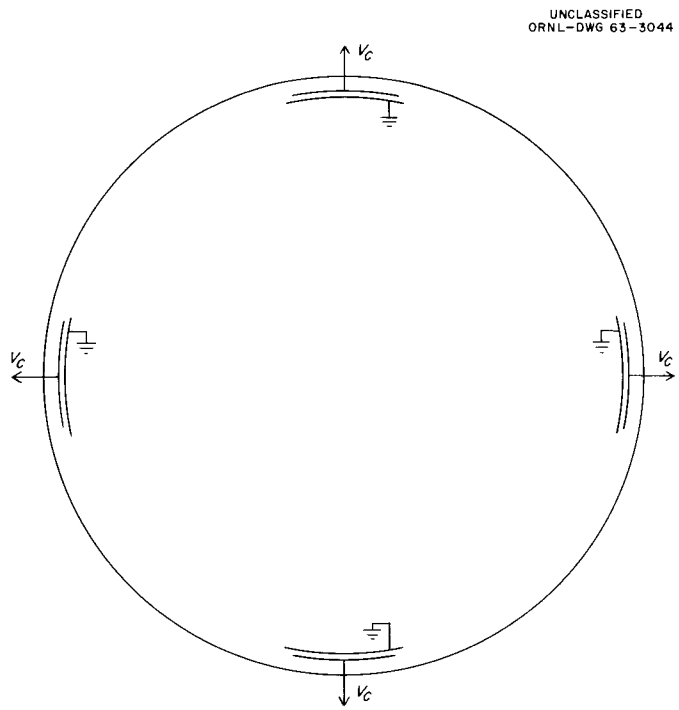

Fig. 19. Possible location of electrodes around machine to produce radial forces on the ions.

In the case of a 'good' isochronous cyclotron in which there is no differential modulation of the main rf voltage with radius, Eq.(23) is modified in the present case to

$$\frac{d\Psi}{dp} = -2\pi m(1-\rho^2)^{3/2}\sin(h\Psi)\frac{N_c e V_c}{2\pi E_o}\frac{L}{S} \tag{47}$$

Here, the signal on the phasing electrode is $\pi/2$ out of phase with respect to the desired phase of the circulating beam. Hence, an ion of the correct phase experiences no net radial force from the phasing electrodes.

The corresponding expression to Eq. (25) is now

$$R_h(\Psi) = \int\frac{\cos\Psi\, d\Psi}{\sin(h\Psi)} = -\int\frac{m^L}{S}\frac{V_c N_c}{V_g N}\, d\rho \tag{48}$$

The trigonometric function can be evaluated in any chosen case but for present purposes it is useful to examine the general nature of the solution.

Substituting ϕ for h Ψ, then

$$R_h(\Psi) = \frac{1}{h} \int \frac{\cos(\phi/h)}{\sin(\phi)} \, d\phi \quad . \tag{49}$$

If the range of integration is restricted to $\phi \pm \pi/2$, then

$$\underset{h=1}{\ln \left|\sin(\phi)\right|} < \underset{\text{increasing } h \longrightarrow}{hR_h(\Psi)} < \underset{h=\infty}{\ln \left|\tan(\phi/2)\right|} \tag{50}$$

Hence, to a first approximation,

$$\left\{\ln \left|\tan(\phi_2/2)\right| - \ln \left|\tan(\phi_1/2)\right|\right\} \simeq hm \frac{N_c L V_c}{N\, S V_g} (\rho_2 - \rho_1) \tag{51}$$

$$= hm \frac{L}{r_o} \frac{V_c N_c}{V_g N} \tag{52}$$

A plot of $\ln \left|\sin(\phi)\right|$ and $\ln \left|\tan(\phi/2)\right|$ is given in Fig. 20 as a function of the angle ϕ. Examination of Eq. (52) and the curves in Fig. 20 indicates that the range of phase focusing in this case is principally over the interval $(+\pi/2h)$ to $(-\pi/2h)$. Within this range there are definite advantages in operating at moderate values of h,

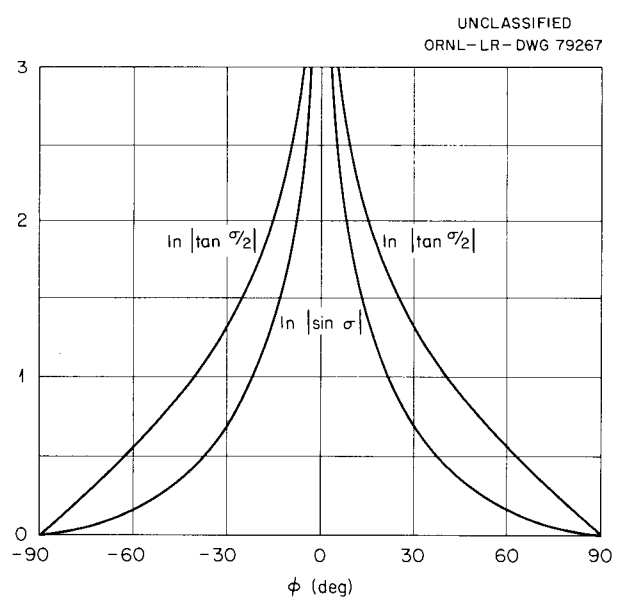

Fig. 20. Curves showing the limiting values of the function $[h\, R_h(\Psi)]$ with ϕ as the variable.

mainly in that for larger h ions are focused more strongly upon $\Psi = 0$. Although this effect is attended by a reduction in the range of usefulness, it is probable that a large range of coverage is not necessary in practice. An attractive feature of this scheme is that ions are focused on an angle which is determined by the relative phasing of the voltages V_c and V_g, and thus is subject to choice.

The application of this scheme to a 'good' isochronous cyclotron would stabilize the system against moderate magnetic and electric field changes, improve the efficiency of extraction, and make possible shorter bursts of particles for time-of-flight experiments. In principle, a tenfold or more decrease in the phase spread could be achieved. For example, if $m = 3$, $h = 4$, $L/r_o = 0.2$, $V_c N_c / V_g N = 1$, and $\Psi_s = 0$, then all ions within the range +15° to -15° would be focused to within $\pm 1.5°$ of Ψ_s.

As shown in Section 5, an energy spread is introduced into the beam at the onset of phase compression. During the phase compression, however, the magnitude of the energy spread is diminished and rapidly becomes of negligible importance.

It is worth noting that in this application no correction is necessary in the main magnetic field, phase compression being available directly on excitation of the necessary electrodes. In practice it is probable that cavities would be used so as to localize the electric fields and to minimize power losses. To assist in the latter point large values of h would be an advantage.

Finally, it may be noted that by reversing the phase of the signal on the electrodes a dispersion of the phases of the ions could be achieved.

Appendix I: The Mean Orbit

An approximate expression is found for the change in mean orbit radius caused by the radial electric impulses arising at the accelerating gaps. Let the geometry of a given orbit be as shown in Fig. 21 where

$$(\phi_1 + \phi_2) = \frac{2\pi}{N} \quad . \tag{1.1}$$

UNCLASSIFIED
ORNL-DWG 63-3045

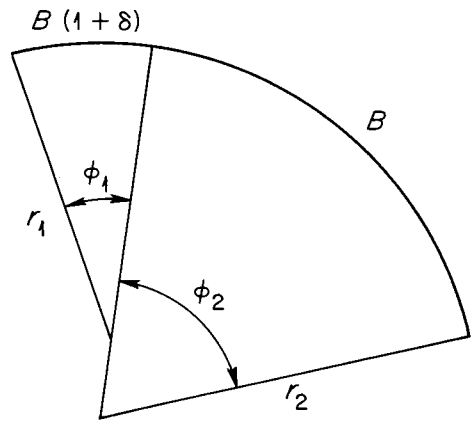

Fig. 21. Construction for determining the change in orbit length as a result of a radial force term.

Here, N is the number of gaps and δ times B is the equivalent magnetic field error of the radial force.

Assuming for the moment that B is independent of the radius, then the period of rotation in the presence of the field error is

$$t = t_0 \left(1 - \frac{N\phi_1 \delta}{(2\pi + \delta)} \right), \tag{1.2}$$

where t_0 is the period when the field error is zero. The value of ϕ_1 is given by

$$\phi_1 = \frac{S_g (1 + \delta)}{\cos \sigma \, r_2}, \tag{1.3}$$

and δ by

$$\delta = \left(\frac{eV_g \sin \sigma}{S_g} \right) \Bigg/ \left(\frac{r_2}{r_0^2} (E_0 + T) \right). \tag{1.4}$$

It follows that

$$\frac{t}{t_0} = \left(1 - \frac{NeV_g \tan \sigma}{2\pi \rho_2^2 (E_0 + T)} \right). \tag{1.5}$$

Let B' be the mean field strength corresponding to the period t and remembering that B is a function of ρ in an isochronous cyclotron, then

$$\frac{t}{t_0} = \frac{B_{iso}}{B'} \tag{1.6}$$

and so, to a good approximation,

$$\frac{B' - B_{iso}}{B'} \simeq \frac{\Delta B}{B_{iso}} = \frac{NeV_g}{2\pi(E_0+T)} \quad \frac{\tan\sigma}{\rho^2} \tag{1.7}$$

But by Eq. (3), this expression is identical with that given in Eq. (11) indicating that the oscillatory components of the radial forces produce little change in the mean orbit radius.

Appendix II: Random Errors

In general, ions will be subject to phase shifts caused by machine imperfections which may vary in time. Slight differences will occur in the magnetic field, for example, each time the magnet is re-energized and changes in the magnet energizing currents will always occur, with attendant phase movements. Mechanical vibration of the rf accelerating electrodes could also produce phase errors. Consequently, the phase history of an ion as it is accelerated to full energy will change in time in a way determined by the sum of the various machine errors.

Let the actual or equivalent magnetic field errors have an average amplitude of ΔB and extend over intervals in (ρ^2) equal to $\Delta(\rho^2)$. The change in phase produced by one such field error in the interval $\Delta(\rho^2)$ is found from Eq. (3.4) in Appendix 3. If it is assummed that the signs of the field errors in successive $\Delta(\rho^2)$ intervals vary in a random way, the probability that an ion has suffered a given phase change after transversing $[\rho^2/\Delta(\rho^2)]$ intervals can be found. By restricting the analysis to zero initial phase angle, the probability that

the sine of the phase angle has a given value after M intervals is given by

$$P_R(n) = \frac{R!}{n!\ (R-n)!\ 2^M} \tag{2.1}$$

where:

$$R = \frac{\rho^2}{\Delta(\rho^2)} , \tag{2.2}$$

$$n = \frac{|\sin \Psi|}{C\Delta(\rho^2)} , \text{ and} \tag{2.3}$$

$$C = \frac{m\pi E_0 \, |\Delta\hat{B}|}{NeV_g \ \hat{B}_0} . \tag{2.4}$$

If the number of intervals is large, Eq. (38) takes the form

$$P_R(n) = \sqrt{\frac{2}{\pi R}}\ e^{-\frac{n^2}{2R}} . \tag{2.5}$$

Differentiation of Eq. (2.5) shows that the probability of n taking a particular value is a maximum when

$$R = n^2 \tag{2.6}$$

From Eqs. (2.2), (2.3), and (2.4) this can be rewritten as

$$|\sin \Psi| = \frac{m\pi E_o}{NeV_g \hat{B}_0} \ |\Delta\hat{B}|_\rho \sqrt{\Delta(\rho^2)} . \tag{2.7}$$

Appendix III: Field Perturbations

The change in phase of an ion caused by a constant mean field error ΔB is found readily in the case of an isochronous cyclotron. From Eq. (14) the phase change per turn is

$$\frac{d\phi}{dp} = 2\pi \frac{\delta\rho}{\rho} = 2\pi(1-\rho^2)^{3/2} \frac{\Delta B}{\hat{B}_0} , \tag{3.1}$$

and from Eqs. (16) and (17), with $\epsilon \equiv \Psi$,

$$\frac{d\phi}{d\rho} = 2\pi \frac{\Delta B}{\hat{B}_0} \frac{E_0}{NeV_g} \frac{\rho}{\cos \Psi} . \tag{3.2}$$

Integrating and including the possibility of operation on the m'th harmonic so that $\Psi = m\phi$, gives

$$\sin \Psi = \frac{\pi \Delta B E_0 m}{\hat{B}_0 N e V_g} \rho^2 . \tag{3.3}$$

Differentiation with respect to (ρ^2) then gives

$$\frac{d(\sin \Psi)}{d(\rho^2)} = \frac{m \pi E_0 \Delta B}{N e V_g \hat{B}_0} , \tag{3.4}$$

where ΔB is assumed constant over the interval considered in (ρ^2).

Appendix IV: Magnetic Fields Associated with RF Cavities

The voltage modulation with radius necessary to produce phase control introduces time dependent rf magnetic fields within the accelerating gaps. These fields can act upon the ions to either assist or oppose the radial forces caused by the cavity electric fields. With reference to Fig. 22, if the gap is also a line of symmetry of the cavity, then the only field components are[6]

$$E_z = (A J_\nu (kr) + B N_\nu (kr)) (C \cos \nu \phi + D \sin \nu \phi) \tag{4.1}$$

and

$$H_\phi = -\frac{1}{k^2} j \omega \varepsilon \frac{\partial E_z}{\partial r} , \tag{4.2}$$

where

$$k = \omega \sqrt{\mu \varepsilon} = \frac{2\pi}{\lambda} . \tag{4.3}$$

Hence, the amplitude of the magnetic field component is

$$H_\phi = \frac{\lambda}{2\pi (377)} \frac{\partial E_z}{\partial r} , \text{ oersteds.} \tag{4.4}$$

For the cavity arrangement in Fig. 22, the rf magnetic fields act so as to increase the effective rate of rise or fall of the electric fields, thereby enhancing the departure of the isophase curve from the gap curve. Another effect of including the rf magnetic fields is that

the isophase curve is no longer phase invariant but moves slightly in space as the phase of an ion varies relative to the rf voltage.

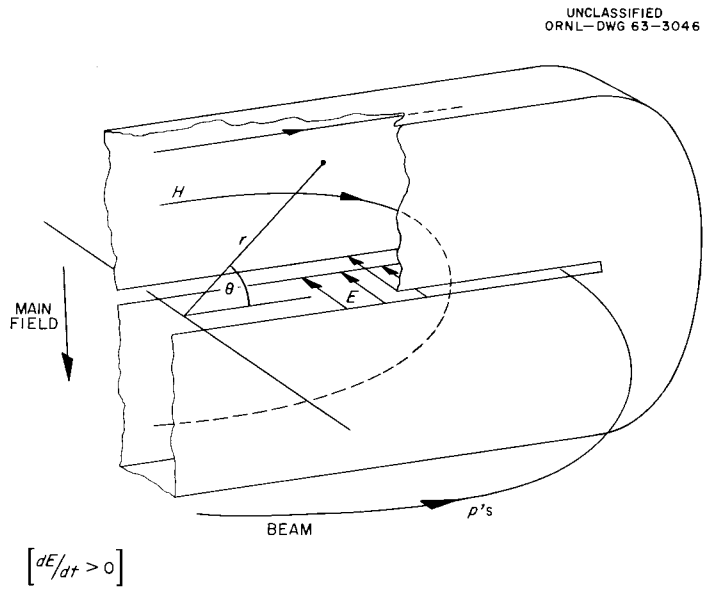

Fig. 22. Fields and coordinates used in describing a radio-frequency cavity resonator.

References

1. Bethe, H. A. and M. E. Rose, Phys. Rev. 52, 1254 (1937).
2. Thomas, L. H., Phys. Rev. 54, 580 (1938).
3. Oak Ridge National Laboratory, Union Carbide Nuclear Company, Oak Ridge, Tennessee. ORNL Report 3324 (1962).
4. Proposal for a Southern Regional Accelerator. Oak Ridge National Laboratory Report CF-57-4-30 (1957).
5. Welton, T. A., Oak Ridge National Laboratory, Private Communication.
6. Ramo, S., and J. R. Whinnery, Fields and Waves in Modern Radio, John Wiley and Sons, Inc. 2nd Ed. (1953).

ORNL-3444
UC-28— Particle Accelerators and
High-Voltage Machines
TID-4500 (26th ed.)

INTERNAL DISTRIBUTION

1. Biology Library
2-4. Central Research Library
5. Reactor Division Library
6-7. ORNL-Y-12 Technical Library
Document Reference Section
8-17. Accelerator Information Center
18-52. Laboratory Records Department
53. Laboratory Records, ORNL R.C.
54. J. E. Beaver
55. C. B. Fulmer
56. F. T. Howard
57. C. E. Larson
58. R. S. Livingston
59. R. S. Lord
60. J. A. Martin
61. S. W. Mosko
62. M. J. Skinner
63. W. R. Smith
64. A. H. Snell
65. J. A. Swartout
66. A. M. Weinberg
67. N. F. Ziegler
68. A. M. Clogston (consultant)
69. B. L. Cohen (consultant)
70. M. Deutsch (consultant)
71. D. L. Judd (consultant)
72. L. J. Rainwater (consultant)
73. J. A. Wheeler (consultant)

EXTERNAL DISTRIBUTION

74-83. F. M. Russell, NIRNS, Rutherford High Energy Laboratory, Chilton, Didcot, Berks. England
84. Research and Development Division, AEC ORO
85-616. Given distribution as shown in TID-4500 (26th ed.) under Particle Accelerators and High-Voltage Machines category (75 copies — OTS)